Synchrotron and Inverse Compton Scattering Radiation from Galactic Dark Matter

Gennaro Miele

University of Naples "Federico II"

Based on the following papers

➢ *Searching for Dark Matter in Messier 33*. E. Borriello, G. Longo, G. Miele, M. Paolillo, B.B. Siffert, F.S. Tabatabaei, R. Beck,
Astrophys.J.709:L32-L38,2010.
e-Print: **arXiv:0906.2013** [astro-ph.HE]

➢ *Secondary radiation from the Pamela/ATIC excess and relevance for Fermi.*
E. Borriello, A. Cuoco, G. Miele,
Astrophys.J.699:L59-L63,2009.
e-Print: **arXiv:0903.1852** [astro-ph.GA]

➢ *Radio constraints on dark matter annihilation in the galactic halo and its substructures.* E. Borriello, A. Cuoco, G. Miele,
Phys.Rev.D79:023518,2009.
e-Print: **arXiv:0809.2990** [astro-ph]

Motivations

➤ Cosmology and Astrophysics provide a striking evidence for DM

➤ Promising candidates for DM particles are the so-called WIMP

➤ WIMPs are realized in SUSY as the Lightest Super-symmetric Particle (LSP) or as the Lightest Kaluka-Klein Particle (LKP)

Dark energy
Dark matter
Neutrinos (Mnu=0.3eV)
Baryons
CMB

0.6%

21.0%

4.4%

74.0%
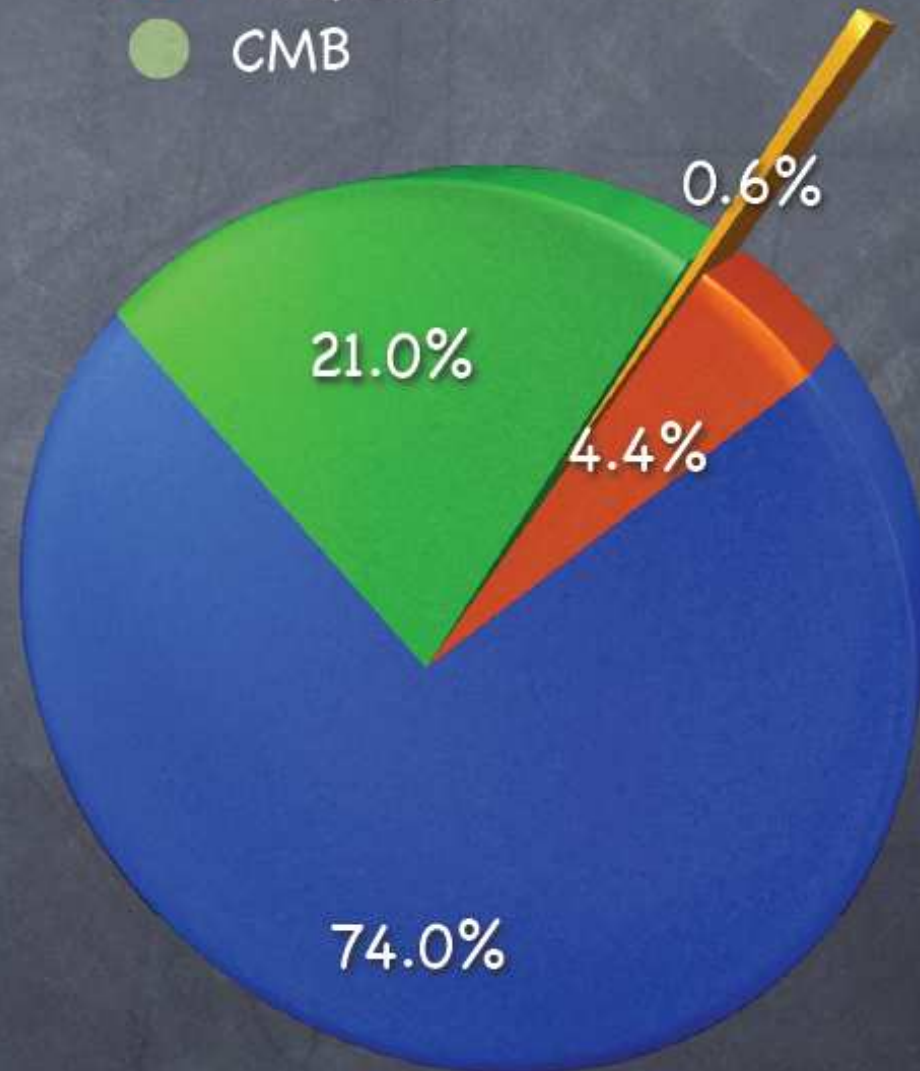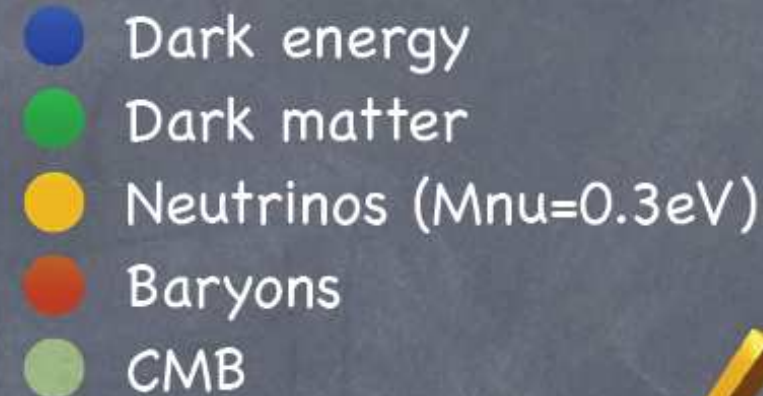
➢ These candidates are self-conjugate thus annihilating in couple produce as final states neutrinos, photons, electrons, light nuclei (as well as their antiparticles) (Indirect DM detection!).

✓ e^+e^- once in the galactic environment, interact with the Galactic Magnetic Field (GMF) and the InterStellar Radiation Field (ISRF).

✓ They will lose energy producing Synchrotron Radiation (SR) in the radio band and Inverse Compton Scattering (ICS) Radiation in the gamma band.
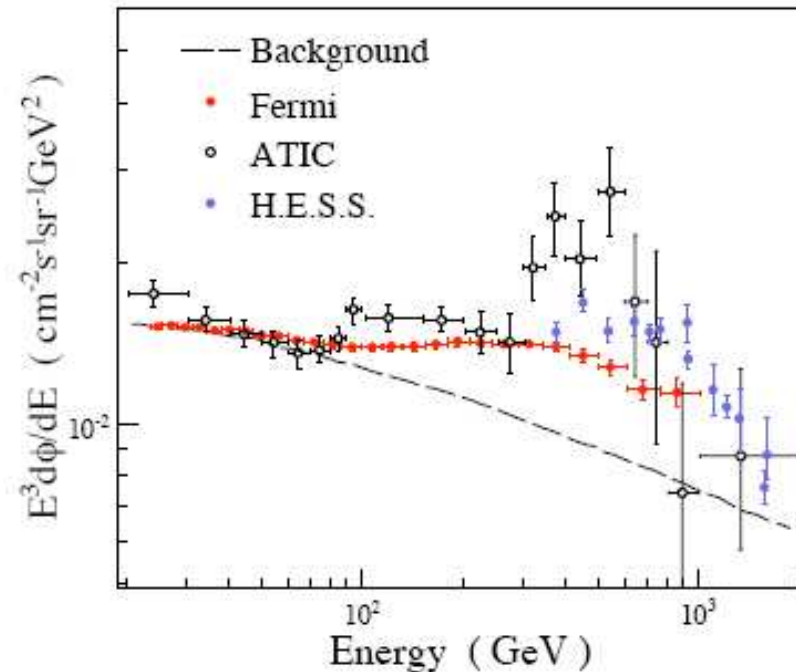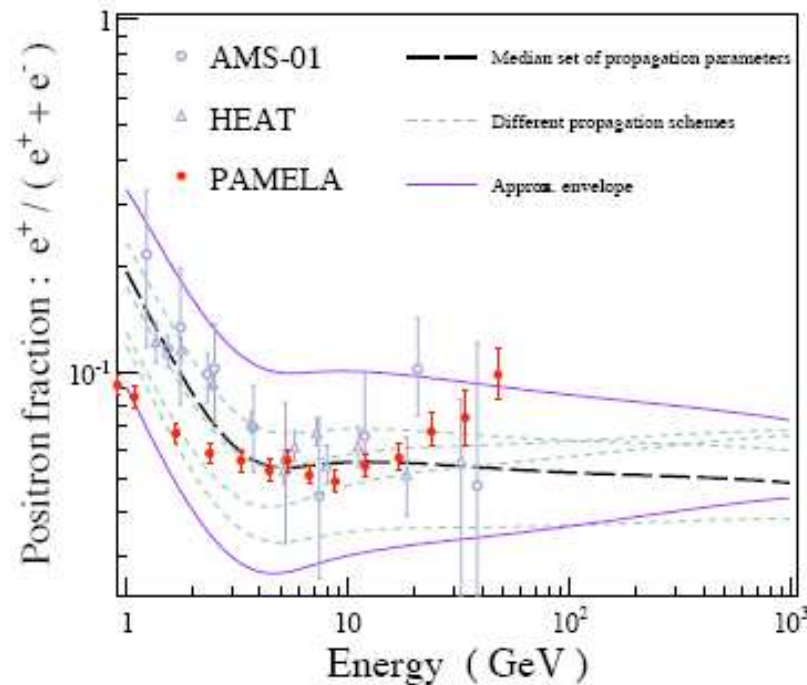
✓ **Need for a Multiwavelength Approach**
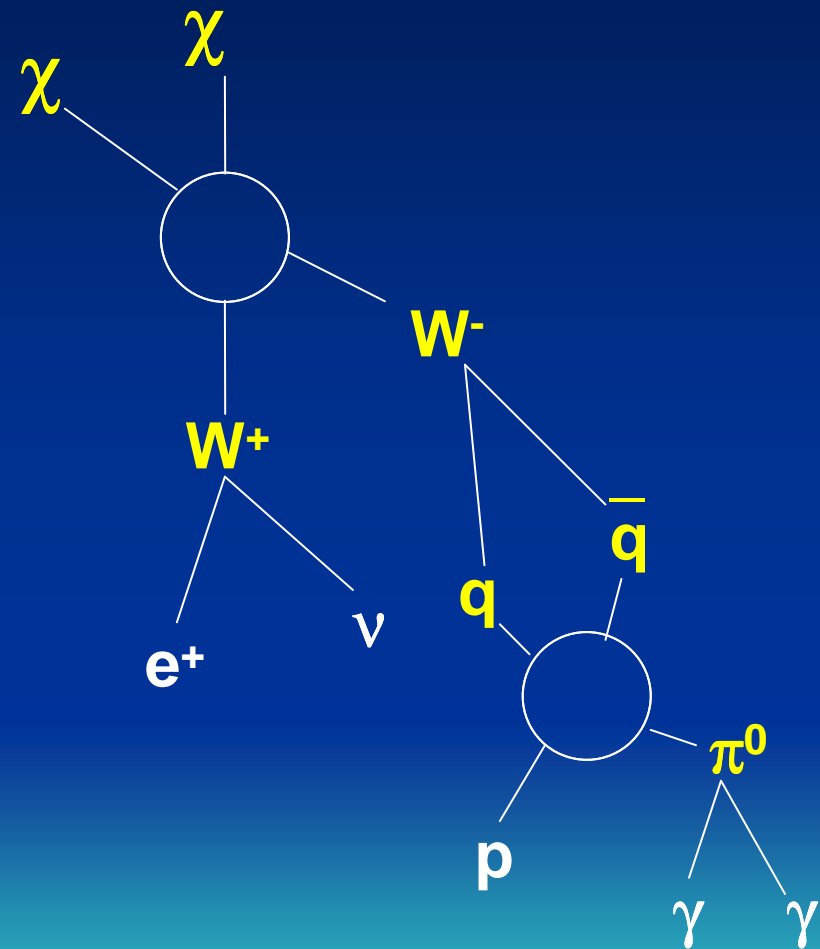
A revival due to the electron/positron puzzle

ATIC – An excess of $e^+ + e^-$ between ~100 GeV and ~ 700 GeV not totally confirmed by Fermi

Pamela – A raise in the positron fraction above 10 GeV until ~ 100 GeV

HESS – A break in the flux is observed

Require a new source of electrons/positrons

Searching for
Radio DM Broadcasting

> Charged leptons and nuclei strongly interact with gas, radiation and Galactic Magnetic Field. During the process of thermalization HE e^+e^- release secondary low energy radiation, in particular in the radio and X-ray band (in principle detectable).

Magnetic lines of force

Synchrotron radiation

Spiralling electron
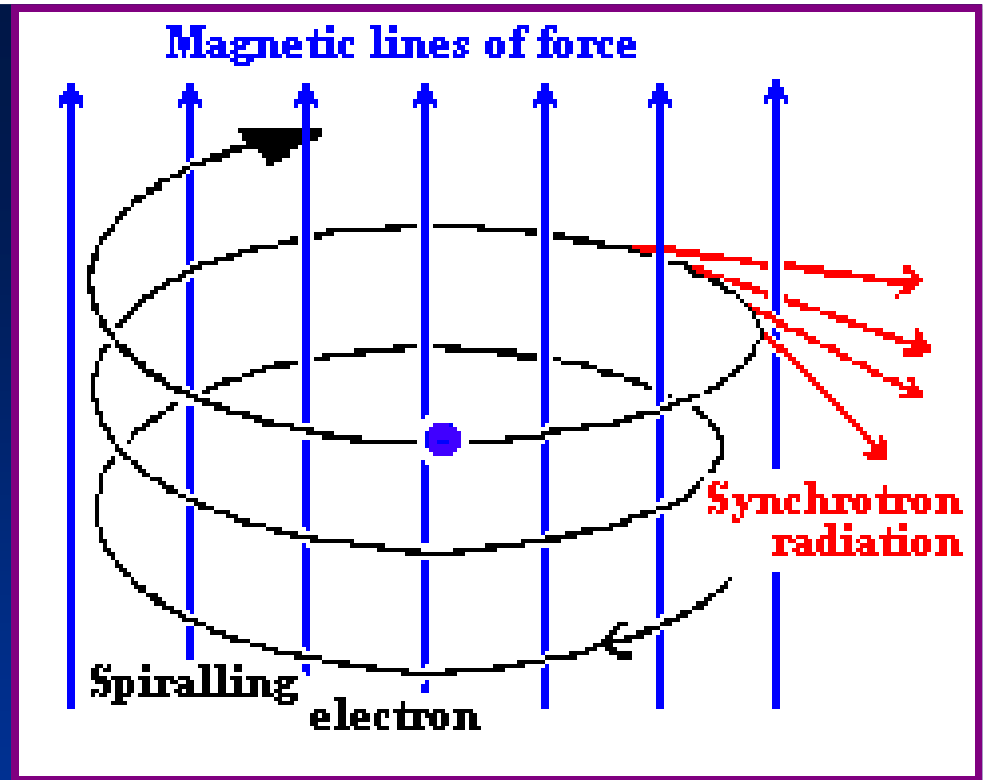
Due to Inverse Compton Scattering on starlight and CMB and Synchrotron on galactic Magnetic Field one gets

$$-\frac{1}{E_e}\left(\frac{dE_e}{dt}\right) = \left(\frac{1}{\tau_{syn}} + \frac{1}{\tau_{ICS}}\right)$$

The two energy loss time scales are

$$\tau_{syn} \cong 4 \cdot 10^{17} \left(\frac{B}{\mu G} \right)^{-2} \left(\frac{E_e}{GeV} \right)^{-1} \text{sec}$$

$$\tau_{ICS} \cong 10^{16} \left(\frac{U_{rad}}{eV/cm^3} \right)^{-1} \left(\frac{E_e}{GeV} \right)^{-1} \text{sec}$$

➤ While the astrophysical uncertainties affecting this signal are similar to the case of direct e⁺e⁻ detection, the sensitivities are quite different and, in particular in the radio band, allows the discrimination of tiny signals even with backgrounds many order of magnitudes more intense.

➤ Interestingly, for Electroweak-Scale DM, the resulting synchrotron radiation falls within the frequency range of WMAP.

Model outline

- **ASTROPHYSICAL INPUTS**
  - ➢ Dark Matter Distribution
  - ➢ Galactic Magnetic Field
  - ➢ Radio Data

- **DM SYNCHROTRON SIGNAL**
  - ➢ Particle Physics
  - ➢ Electrons equilibrium distribution
  - ➢ Synchrotron spectrum

- **DM ANNIHILATION CONSTRAINTS**

Dark Matter Distribution

Our knowledge of the DM spatial distribution on galactic and subgalactic scales has greatly improved thanks to recent high resolution zoomed N-body simulations. The galactic halo seems very well described by the Navarro-Frank-White (NFW) distribution (conservative point of view)

$$\rho(r) = \frac{\rho_h}{\dfrac{r}{r_h}\left(1 + \dfrac{r}{r_h}\right)^2}$$

Beside the smooth halo component DM is also distributed into a clumpy component with the two total masses ~ of the same order of magnitude

We will assume an universal NFW profile for the mass spectrum number density of subhaloes, in galactocentric coordinates

Galactic Magnetic Field

The MW magnetic field is still quite uncertain especially near the galactic center. The overall structure is generally believed to follow the spiral pattern of the galaxy itself with a normalization of about $\sim 1 \ \mu$G near the solar system. A toroidal or a dipole component is considered in some model.

We use a typical spiral pattern (Tinyakov and Tkachev model) with an exponential decreasing along the z axis and a 1/r behavior in the galactic plane. The field intensity in the inner kpc's is constant to about 7 μG.

astro-ph/0510444
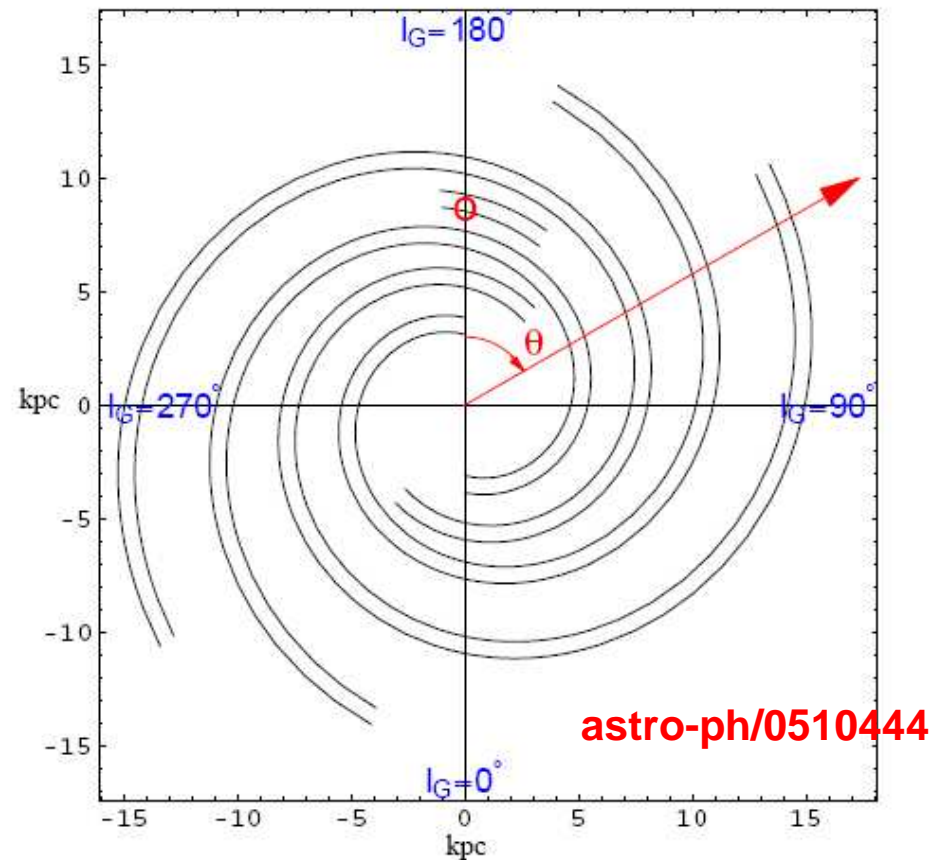
Radio Data

Constraints on the DM emission are obtained comparing the expected diffuse emission from the "smooth halo" and the unresolved population of "clumps" with all sky observation in the radio band. In the frequency range between 100 MHz-100 GHz where the DM synchrotron signal is expected

Competing synchrotron emission is given by

• Cosmic Ray electrons accelerated in supernovae shocks, dominate up to ∼ 10 GHz.

• At higher frequencies CMB and its anisotropies represent the main signal.

Thanks to the very sensitive multi-frequency survey by the WMAP (22.8, 33.0, 40.7, 60.8 and 93.5 GHz), this signal can be modeled and thus removed from the observed radio galactic emission.

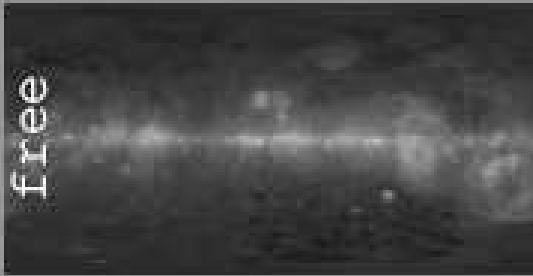Other processes contributing in the 10-100 GHz range
- Synchrotron Radiation (low energy)
- Thermal bremsstrahlung (free-free emission) of electrons on the galactic ionized gas (low energy)
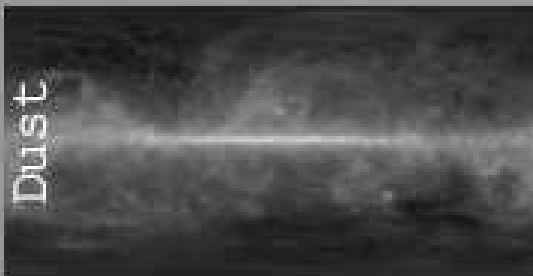- Emission by small grains of vibrating or spinning dust (high energy)

Synchrotron

Free-free

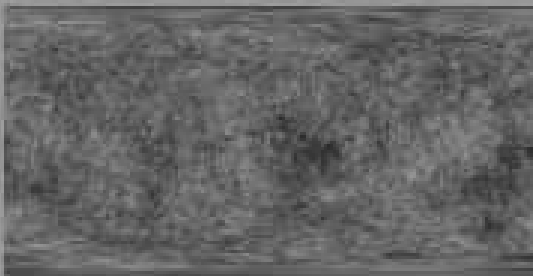T & S Dust

CMB

Dan Hooper - *Dark Matter Annihilations in the WMAP Sky*
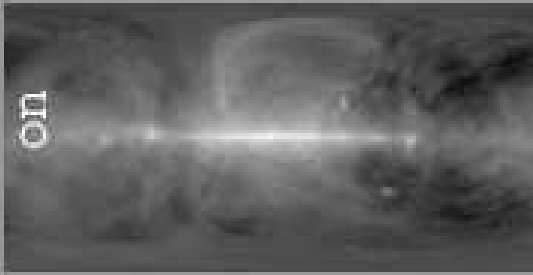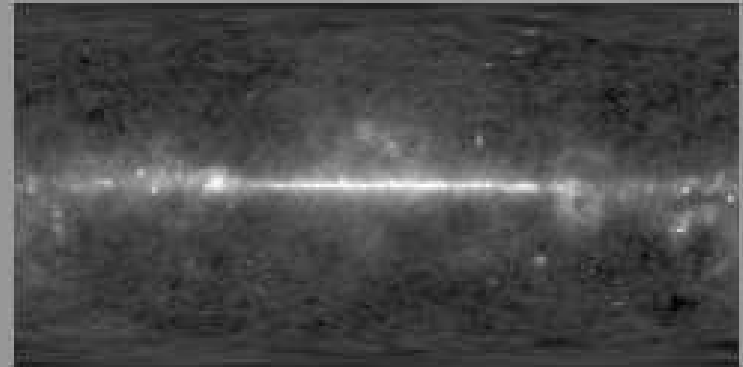
WMAP

Well, actually... No

Sky map of galactic foregrounds at 23 GHz

Radio Sky at 23 GHz

$-18.$ ▬▬▬ $-14.$ Log (GeV cm^{-2} s^{-1} Hz^{-1} sr^{-1})
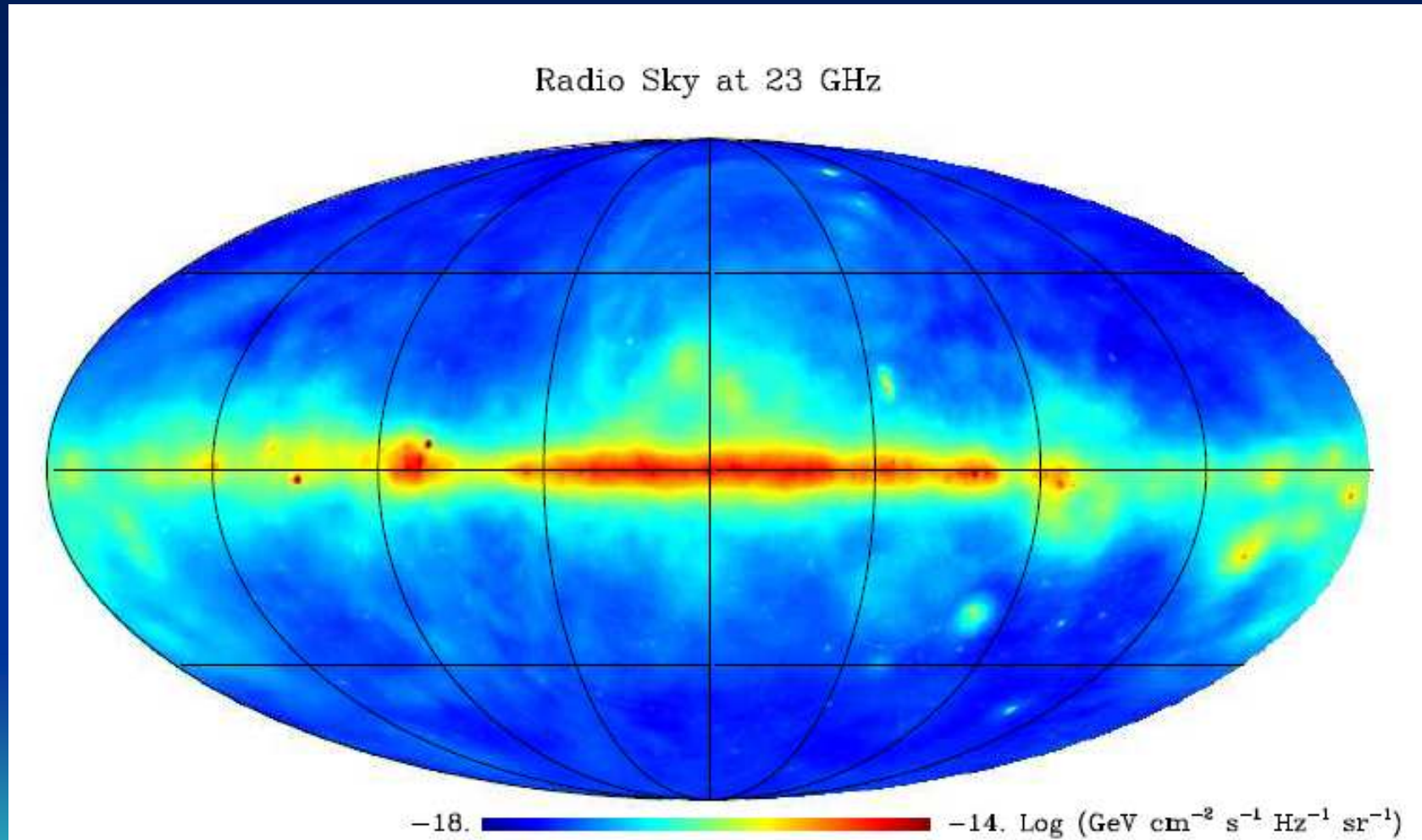
Residual map showing the WMAP Haze at 23 GHz

WMAP Haze at 23 GHz

-21.8 ▮▮▮▮▮▮▮▮▮▮▮ -15.8 Log (GeV cm^{-2} s^{-1} Hz^{-1} sr^{-1})
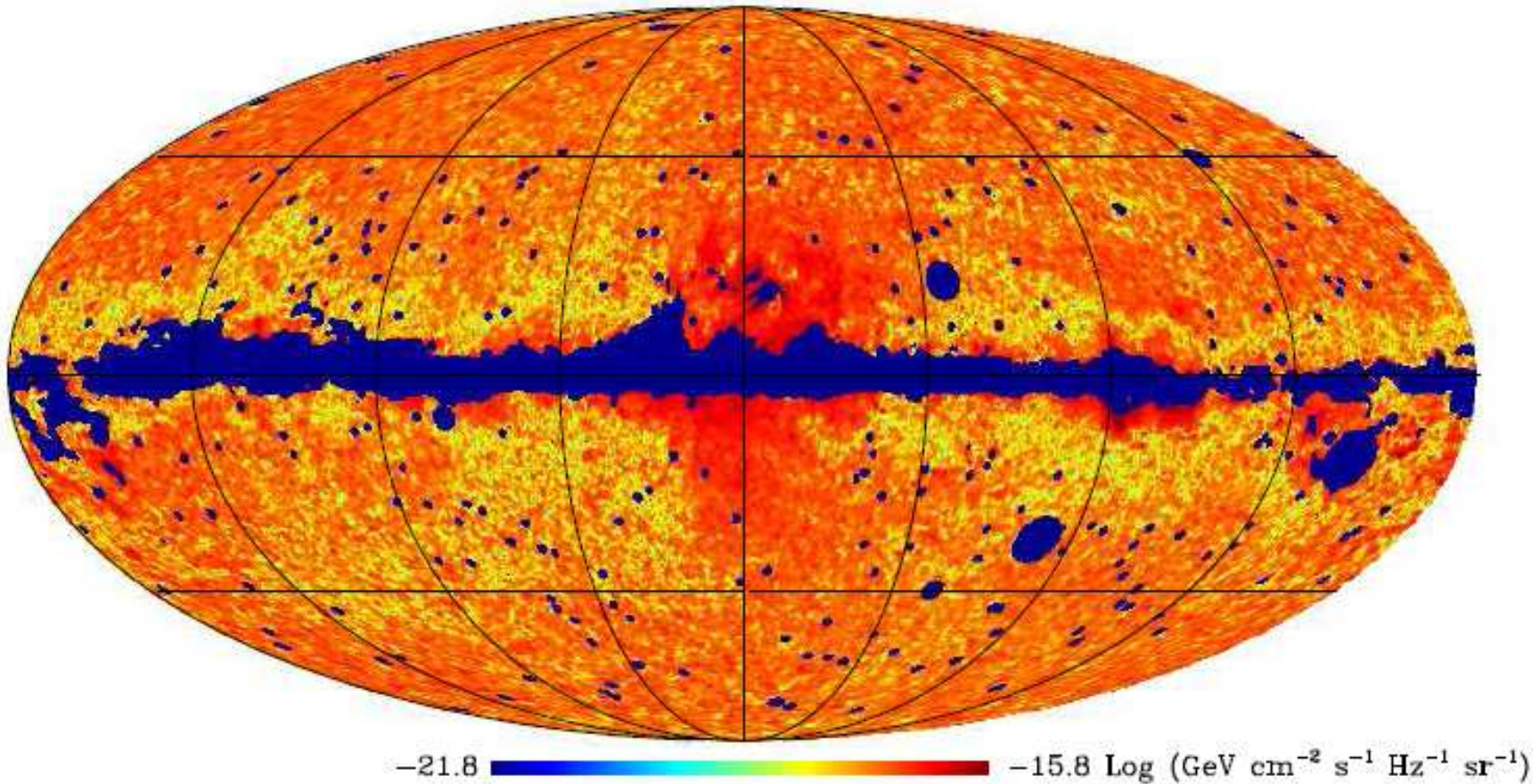
Our approach:

To compare the DM signal with the observed radio emission where only the CMB is modeled and removed. For this purpose we have used the code described in arXiv:0802.1525[astro-ph] where most of the radio survey observations in the range 10 MHz - 100 GHz are collected and a scheme to derive interpolated, CMB cleaned sky maps at any frequency in this range is described.

We consider a χ mass range of $50 \text{ GeV} \lesssim m_{\chi} \lesssim 500 \text{ GeV}$ and $\langle \sigma_A v \rangle = (10^{-26} - 10^{-21}) \text{ cm}^3 \text{ s}^{-1}$

$$\chi + \chi \longrightarrow q + \bar{q} \longrightarrow \pi^{\pm} + X$$

$$\longrightarrow \nu_{\mu} + \mu^{\pm}$$

$$\longrightarrow \nu_e + \nu_{\mu} + e^{\pm}$$

Neutralinos mainly annihilate in the hadronic channel

$$\frac{\mathrm{d}N_e}{\mathrm{d}E_e}(E_e) = \int_{E_e}^{m_\chi c^2} \mathrm{d}E_\mu \frac{\mathrm{d}N_e^{(\mu)}}{\mathrm{d}E_e}(E_e, E_\mu)$$

$$\times \int_{E_\mu}^{E_\mu/\xi} \mathrm{d}E_\pi W_\pi(E_\pi) \frac{\mathrm{d}N_\mu^{(\pi)}}{\mathrm{d}E_\mu}(E_\pi)$$

with $\xi = (m_\mu/m_\pi)^2$, where

$$\frac{\mathrm{d}N_e^{(\mu)}}{\mathrm{d}E_e}(E_e, E_\mu) = \frac{2}{E_\mu}\left[\frac{5}{6} - \frac{3}{2}\left(\frac{E_e}{E_\mu}\right)^2 + \frac{2}{3}\left(\frac{E_e}{E_\mu}\right)^3\right],$$

$$\frac{\mathrm{d}N_\mu^{(\pi)}}{\mathrm{d}E_\mu}(E_\pi) = \frac{1}{E_\pi}\frac{m_\pi^2}{m_\pi^2 - m_\mu^2},$$

$$W_\pi(E_\pi) = \frac{1}{m_\chi c^2}\frac{15}{16}\left(\frac{m_\chi c^2}{E_\pi}\right)^{\frac{3}{2}}\left(1 - \frac{E_\pi}{m_\chi c^2}\right)^2$$

Electron Equilibrium Distribution

Dark matter annihilation injects electrons in the galaxy at the constant rate

$$Q(E_e, r) = \frac{1}{2}\left(\frac{\rho(r)}{m_\chi}\right)^2 \langle \sigma_A v \rangle \frac{dN_e}{dE_e}$$

The injected electrons loose energy in the interstellar medium and diffuse away from the production site.

$$\frac{\partial}{\partial t}\frac{dn_e}{dE_e} = \vec{\nabla} \cdot \left[K(E_e, \vec{r})\vec{\nabla}\frac{dn_e}{dE_e}\right] + \frac{\partial}{\partial E_e}\left[b(E_e, \vec{r})\frac{dn_e}{dE_e}\right]$$
$$+ Q(E_e, \vec{r}),$$

The diffusion length of electrons is generally of the order of a kpc thus for the diffuse signal generated all over the galaxy, spatial diffusion can be safely neglected. This is not the case for the signal coming from a single clump for which the emitting region is much smaller than a kpc.

# Neglecting spatial diffusion, steady state solution reads

$$\frac{dn_e}{dE_e}(E_e, \vec{r}) = \frac{\tau}{E_e} \int\limits_{E_e}^{m_\chi c^2} dE\, Q(E, \vec{r})$$

where τ is the cooling time resulting from the sum of several energy loss processes: Synchrotron emission and Inverse Compton Scattering (ICS) on the background photons (CMB and starlight) only **$1/\tau = 1/\tau_{syn} + 1/\tau_{ICS}$**

$$\tau(E_e, \vec{r}) = \left(\frac{E_e}{GeV}\right)^{-1} \mu(\vec{r})\, 9.82\, 10^{15}\, s$$

$$\mu(\vec{r}) = \left[\left(\frac{B(\vec{r})}{\mu G}\right)^2 + 40.2 \frac{U_{rad}(\vec{r})}{eV/cm^3}\right]$$

Other processes, like synchrotron self absorption (ICS on the synchrotron photons), e^+e^- annihilation, Coulomb scattering over the galactic gas and bremsstrahlung are generally slower. They can become relevant for extremely intense MF.

Projections of the galaxy in the *xy* and *xz* planes showing the fractional synchrotron contribution to the *e*± total energy losses for TT model of GMF and Galprop model of ISRF. The synchrotron losses contribute up most to 20% reaching its maximum at the center of the magnetic arms. In the remaining regions, included the galactic center, ICS is dominating.
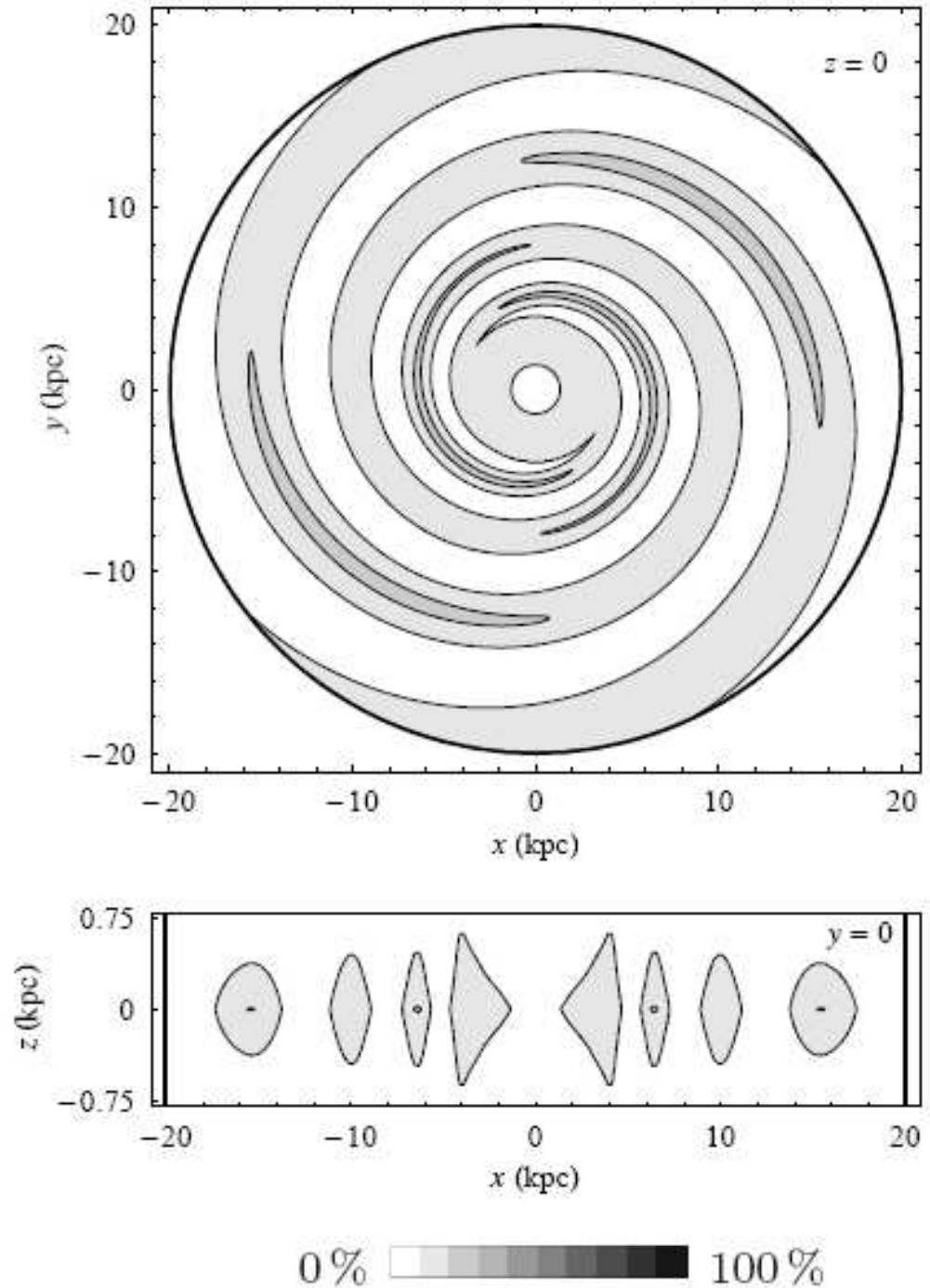
Synchrotron spectrum

The synchrotron spectrum of an electron gyrating in a magnetic field has prominent peak at the resonance frequency

$$\nu = 3.7 \left(\frac{B}{\mu G} \right) \left(\frac{E_e}{GeV} \right)^2 MHz$$

Using this *frequency peak* approximation, the *synchrotron emissivity* can be defined as

$$j_\nu(\nu, \vec{r}) = \frac{dn_e}{dE_e}\left(E_e(\nu), \vec{r}\right) \frac{dE_e(\nu)}{d\nu} \frac{E_e(\nu)}{\tau_{syn}}$$

Summing the smooth halo and clump distribution terms one gets

$$j_\nu^{\mathrm{DM}} = \frac{1}{4}\left(\frac{m_\chi c^2}{\mathrm{GeV}}\right)^{-3}\frac{\langle\sigma_{\mathrm{A}}v\rangle}{\mathrm{cm}^3\mathrm{s}^{-1}}\left\{\left[\frac{\rho_{\mathrm{h}}/\mathrm{GeV}c^{-2}\mathrm{cm}^{-3}}{(r/r_{\mathrm{h}})(1+r/r_{\mathrm{h}})^2}\right]^2 + \frac{\rho_{\mathrm{CL}}/\mathrm{GeV}c^{-2}\mathrm{cm}^{-3}}{(r/r_{\mathrm{h}})(1+r/r_{\mathrm{h}})^2}\right\}$$

$$\mu(\vec{r})\sum_k A_k(m_\chi)\left(\frac{B(\vec{r})}{\mu\mathrm{G}}\right)^{1-k/2}\left(\frac{\nu}{\mathrm{Hz}}\right)^{k/2}\mathrm{GeV}\,\mathrm{cm}^{-3}\mathrm{s}^{-1}\mathrm{Hz}^{-1}\mathrm{sr}^{-1}.$$

Interestingly, from the point of view of DM annihilation the unresolved clumps signal behaves like a further smooth NFW component with the same scale radius of the halo profile, but with a different *effective density*

Sky map of the galactic radio signal generated by the DM smooth halo at the frequency of 1 GHz.

DM synchrotron at 1 GHz
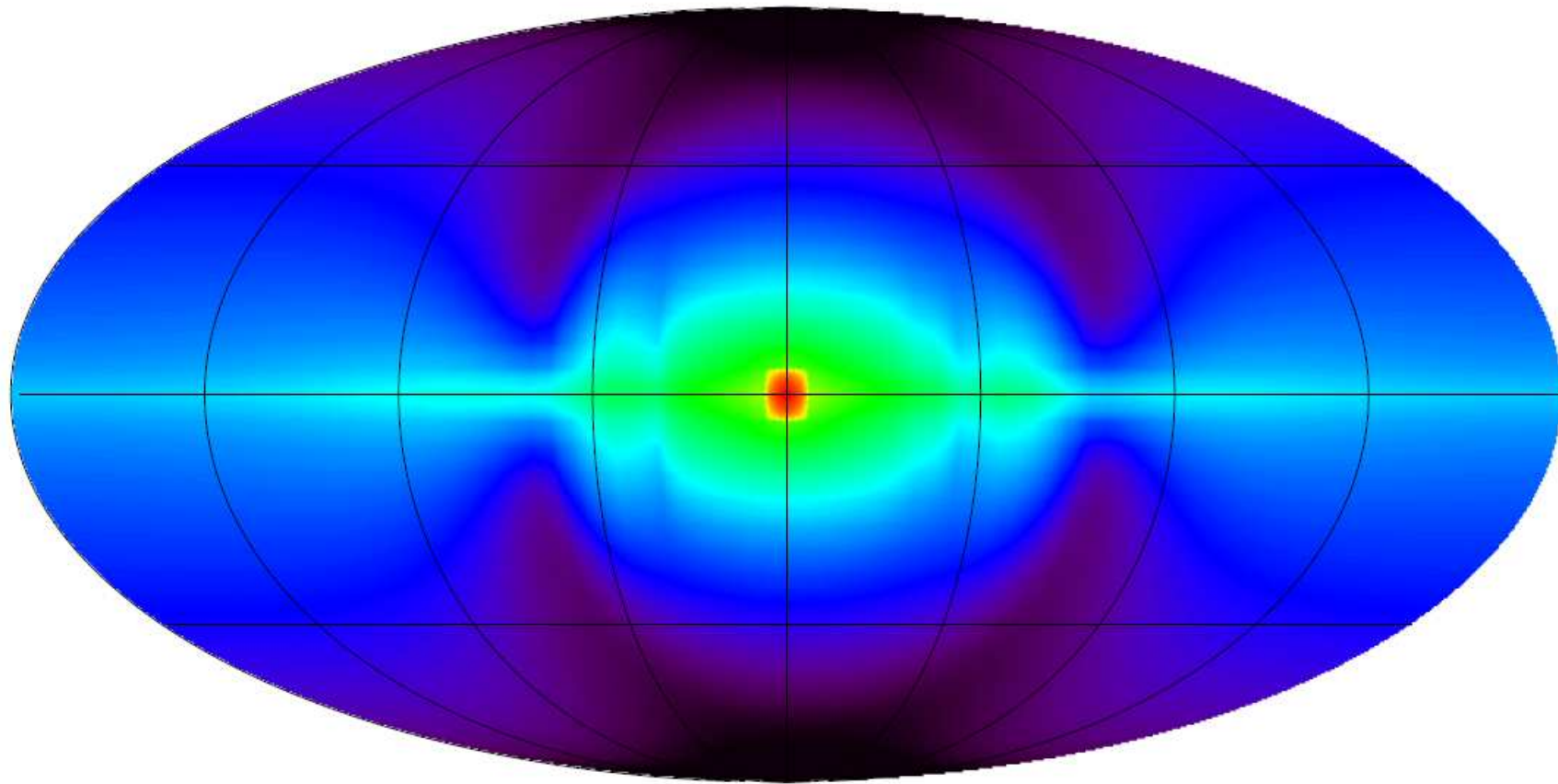
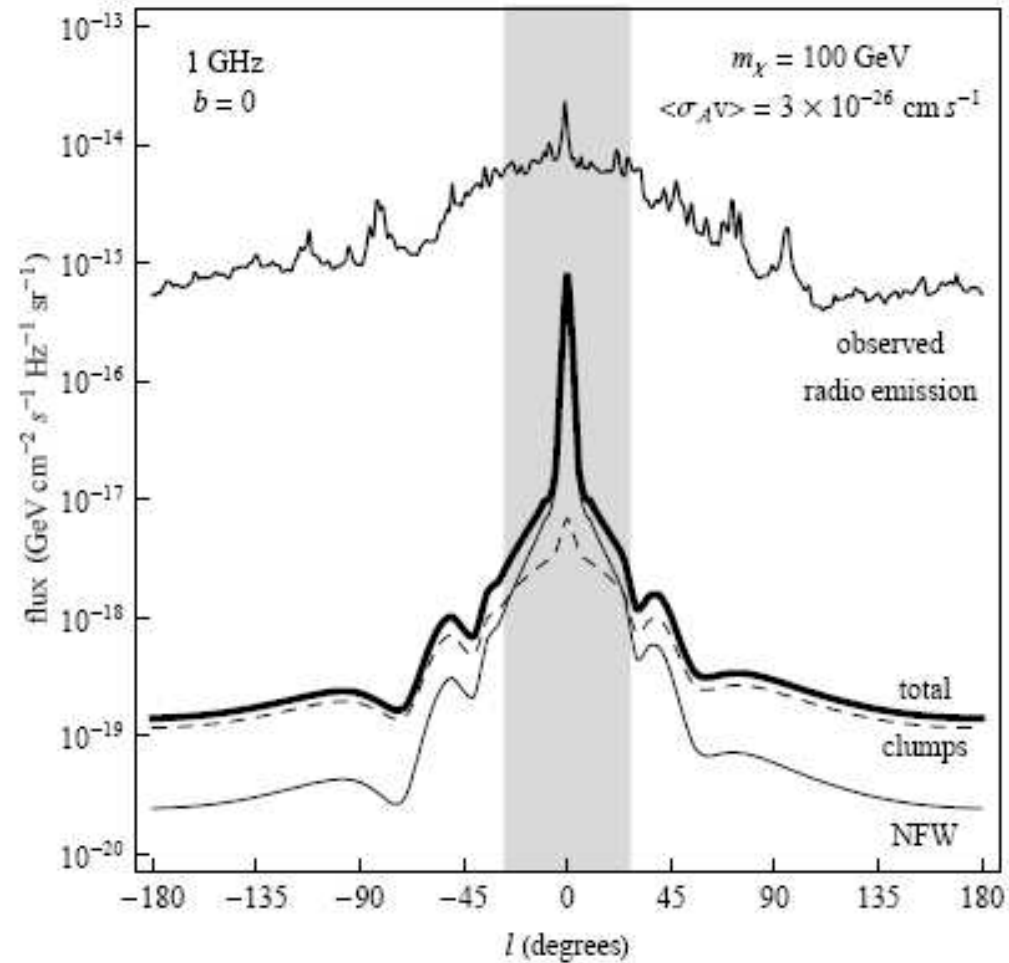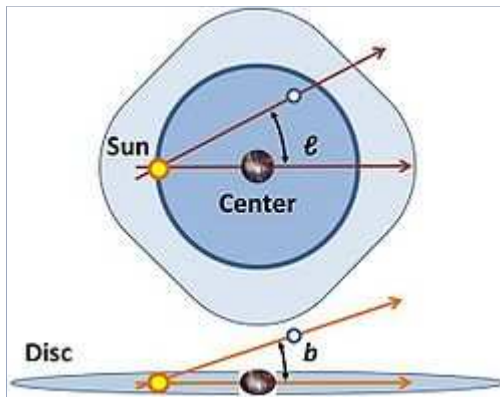-21.1 ▬▬▬▬▬ -15.1 Log (GeV cm^{-2} s^{-1} Hz^{-1} sr^{-1})

FIG. 6: DM synchrotron profile for the Halo and unresolved substructures and their sum at 1 GHz for $m_\chi = 100$ GeV and $\langle \sigma_A v \rangle = 3 \times 10^{-26}$ cm^{3}s^{-1}. The astrophysical observed emission at the same frequency is also shown.

DM ANNIHILATION CONSTRAINTS

In the analysis we use a small mask covering a $15^0 \times 15^0$ region around the galactic center where other energy loss processes are at work
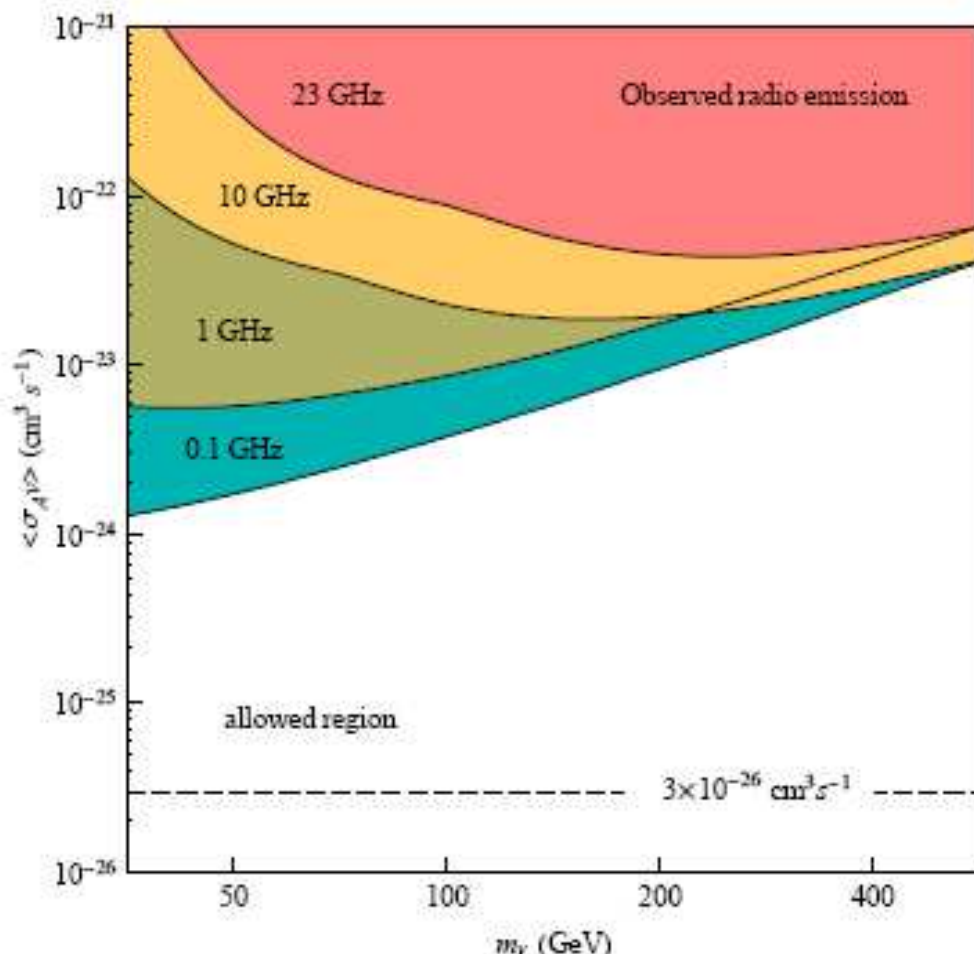
Esclusion plot in the m_χ - $\langle \sigma_A v \rangle$ plane. Assuming no dominant DM synchrotron emission. No foreground sub.
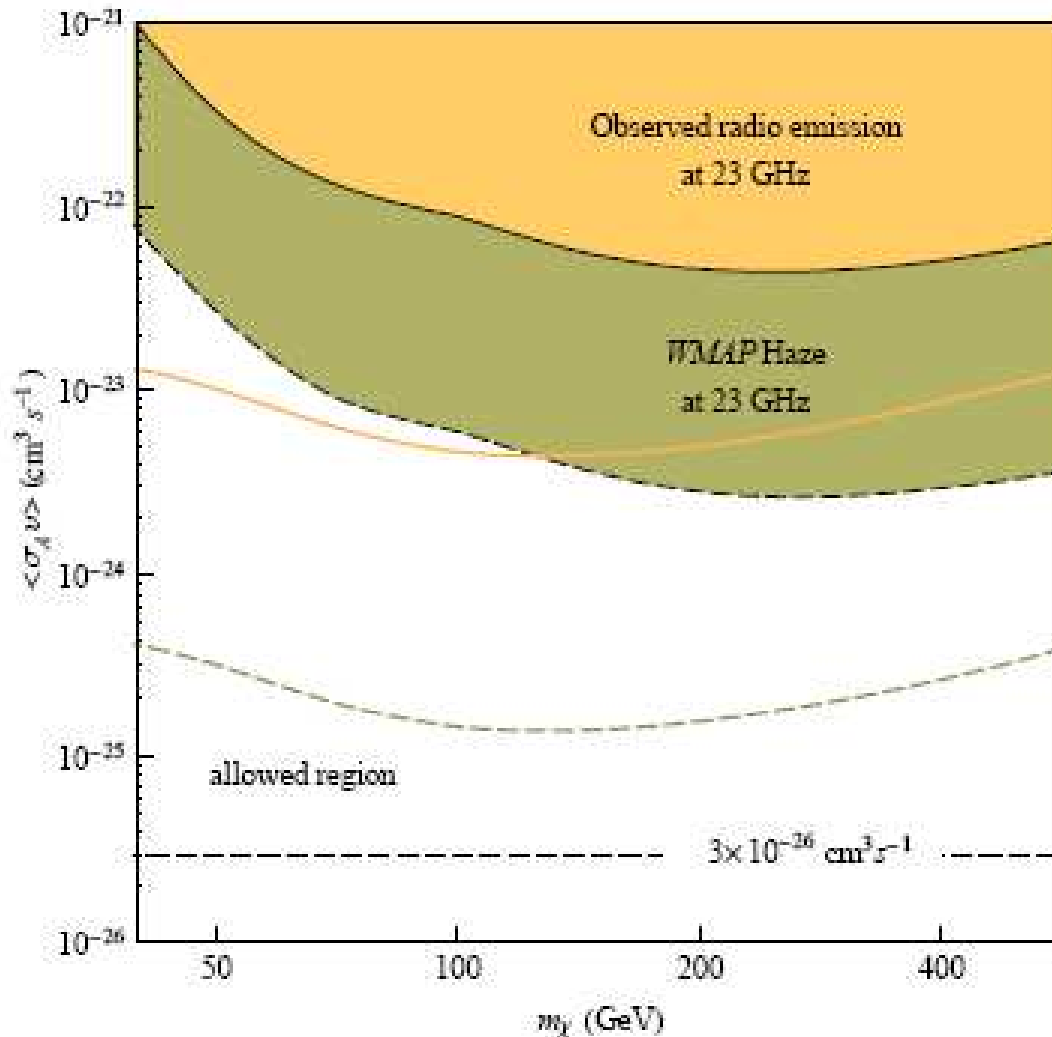
*Esclusion plot in the m_χ - $<\sigma_A v>$ plane.* Constraints from the WMAP 23 GHz foreground map and 23 GHZ foreground cleaned residual map (the WMAP Haze) for the TT model of MF (filled regions) and for a uniform 10 μG field (dashed lines)

Results for MW

- The use of the haze at 23 GHz gives about one order of magnitude better constraints with respect to the synchrotron foregrounds at the same frequency.

- The information at other frequencies are complementary giving better constraints at lower DM masses. The constraints improve of about one order of magnitude at m_χ = 100 GeV from 23 GHz to 1 GHz while only a modest improvement is achieved considering further lower frequencies as 0.1 GHz.

- To further improve the bounds is difficult because

  i) of the removal procedure of foreground contribution from the radio continuum

  ii) of the integration along the line of sight which prevents a proper estimate of the local values of both galactic magnetic field and radio continuum emission.

To overcome such problems we will reapply the analysis to the nearby, close to face-on, galaxy Messier 33 (M33)
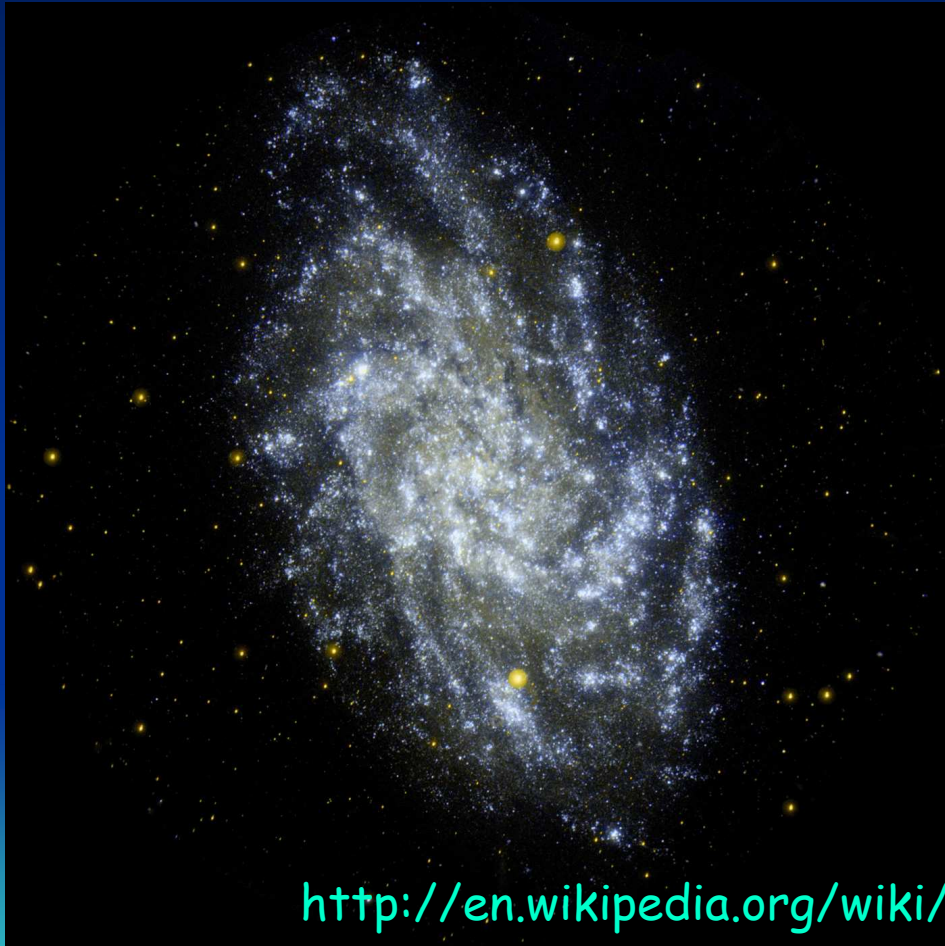
The **Triangulum Galaxy** is a spiral galaxy approximately 3 million light years (ly) distant in the **constellation Triangulum**. It is catalogued as **Messier 33** or **NGC 598**, and is sometimes informally referred to as the *Pinwheel Galaxy*, a moniker it shares with Messier 101. The Triangulum Galaxy is a member of the **Local Group** of galaxies, which includes the **Milky Way Galaxy**, the **Andromeda Galaxy** and about **30 other smaller galaxies**. M33 has been extensively studied at all wavelengths

http://en.wikipedia.org/wiki/Triangulum_Galaxy

Remarkably: it is characterized by regions of a particularly low level of radio emissivity (*radio cavities*)
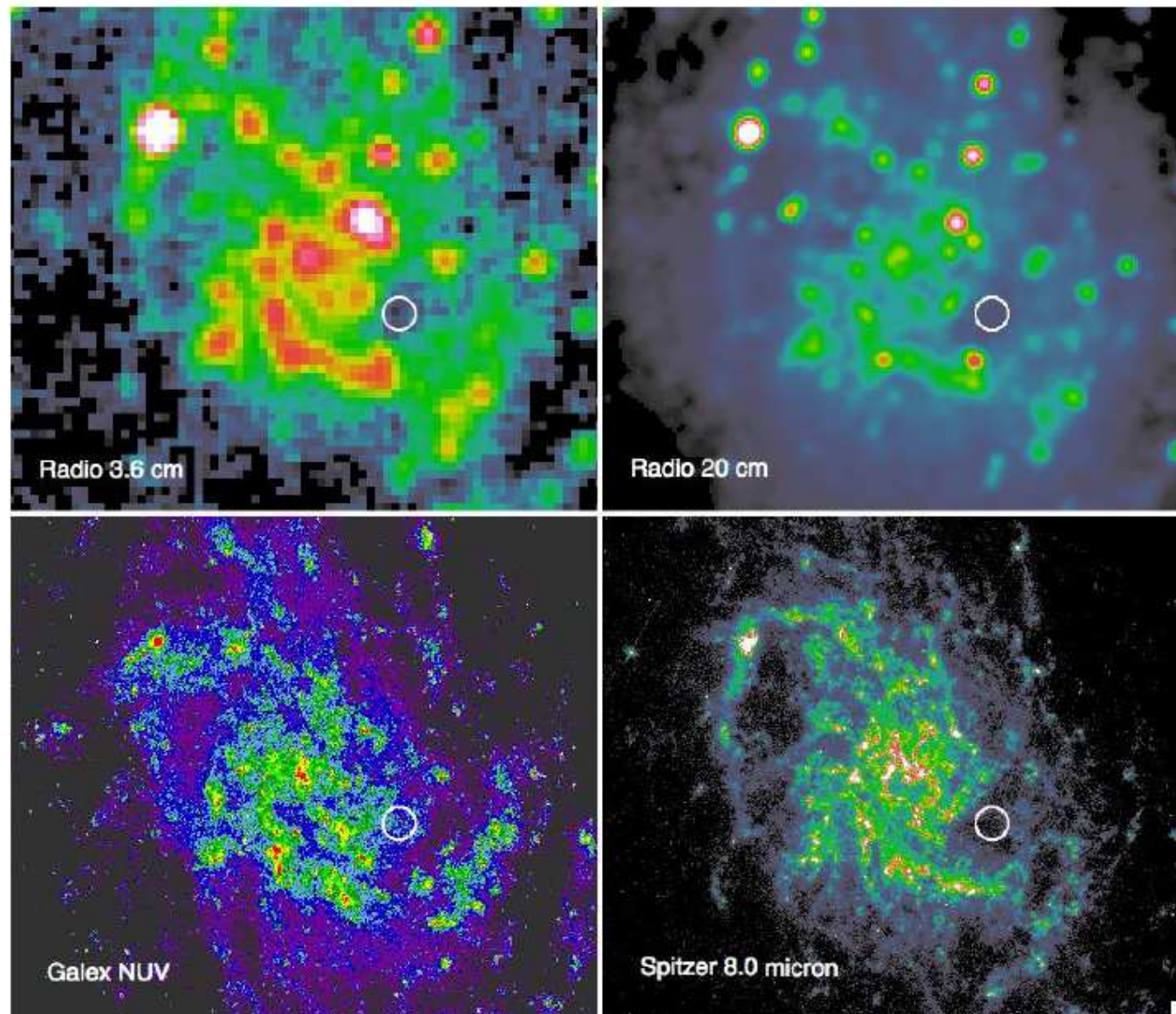

Figure 2. Emission from M33 at different wavelengths. From the upper left clockwise: radio continuum at 3.6 cm, radio continuum at 20 cm, far infrared at 8.0 μm (data from Spitzer telescope), and near-UV at 2300 Å. The *radio cavity* is marked by a circle.

- The most noticeable feature, marked as a circle, is the interarm cavity located at R.A. $1^h 33^m 24^s.0$ and decl. $30° 35' 39.0''$, i.e., at 2.1 kpc from the center.

- This cavity has an area of $\sim 5 \times 10^3$ arcsec^2 and it is resolved at all wavelengths

- It is not yet possible to uniquely determine the DM density of M33, nonetheless both a cored and a spiked profile can be deduced fitting the galaxy rotation curve. We have checked the following two profiles as relevant examples of the above classes

$$\rho(r) = \left(\frac{r}{r_0}\right)^{-1}\left(1+\frac{r}{r_0}\right)^{-2}\rho_0$$

$$\rho(r) = \left(1+\frac{r}{r_0}\right)^{-1}\left[1+\left(\frac{r}{r_0}\right)^2\right]^{-1}\rho_0$$

Table 1
DM Density Distribution Parameters

Model	r_0 (kpc)	ρ_0 (GeV c^{-2} cm^{-3})
NFW	35	0.0574
Burkert	12	0.420

Magnetic Field

Following Tabatabaei et al. (2008), the equipartition total magnetic field strength in the radio cavity is estimated as 7.1 ± 0.5 μG. An exponential decrease is assumed to describe the field along the z-axis:

$$B = B_0 \, e^{-|z|/z0}$$

where $z_0 \sim 7$ kpc. If the equipartition hypothesis were not valid the situation would be more involved:

• 1. If the field strength is constant across the cavity, the CR Electrons have to be deficient to explain the low radio emission. We estimated a 7.5 μG field strength in this case and a scale height that could vary from 5 to 10 kpc;

• 2. If however the CRE density is about constant across the cavity, the field there would be smaller than 7 μG . We estimated $B \sim 3.2\mu$G and $z_0 = 3.5$ kpc.

InterStellar Radiation Field

According to Deul (1989) we assume for the ISRF in the disk of M33

$$U_{\text{rad}}(R) = 5.32 \, e^{-R/2.10} \, \chi$$

where $\chi = 0.539$ eV cm^{-3} is the MW's ISRF at the solar system position. The previous expression is obtained by setting the ISRF equal to χ to a galactocentric radius of 3.5 kpc. To deduce the scale height of the exponential decrease of the ISRF far from the disk, we rescale the MW field in the same way. Thus we get for the radio cavity

$$U_{\text{rad}}(z) = U_0 \, e^{-|z|/h0}$$

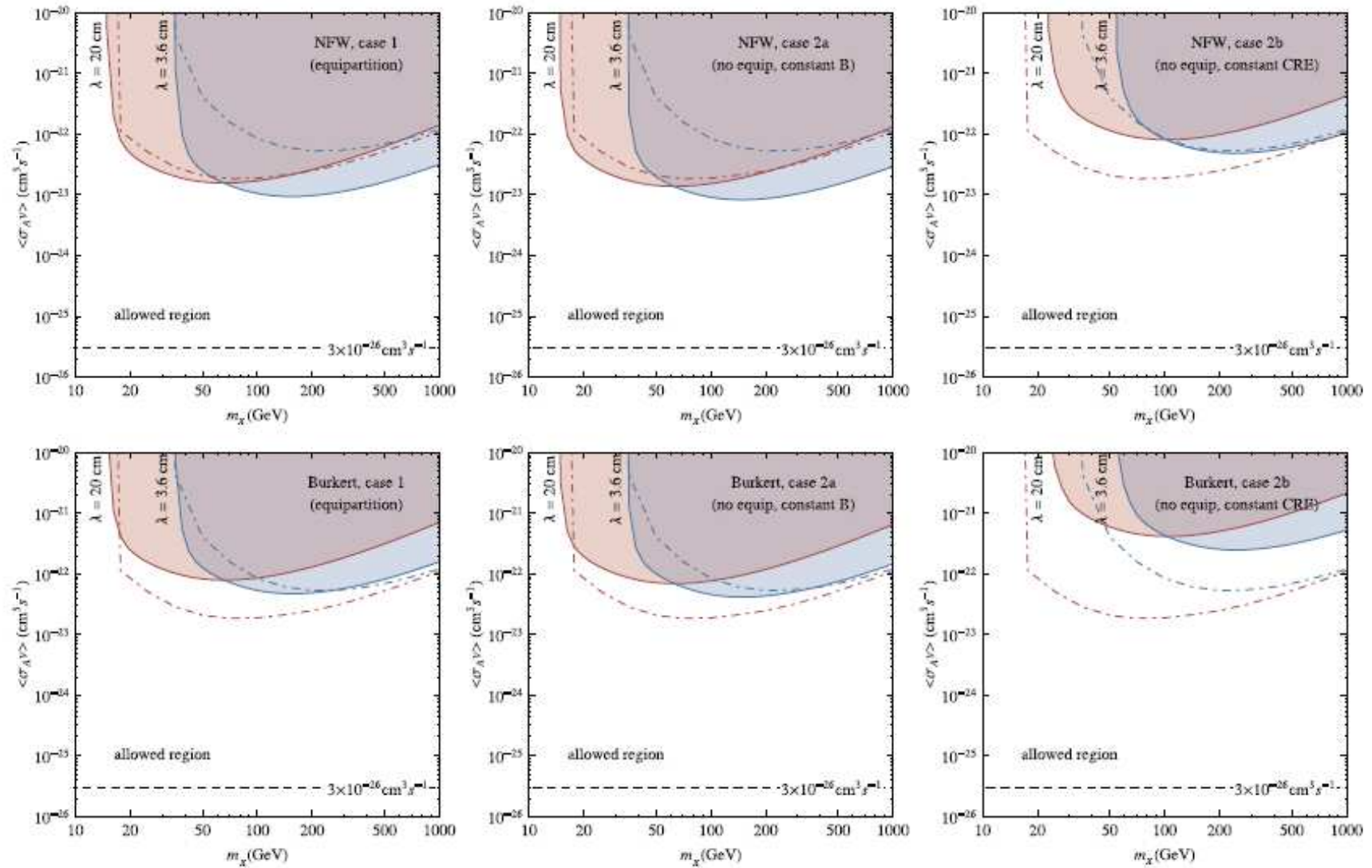with $U_0 = 1.05$ eV cm^{-3} and $h_0 = 1.53$ kpc.

Figure 3. Constraints in the $m_\chi - \langle \sigma_A v \rangle$ plane from radio observation of the *radio cavity* of M33 at 3.6 and 20 cm. Full annihilation into $b\bar{b}$ couples is assumed. The upper panels refer to a NFW DM density profile, the lower ones to a Burkert profile. Three cases are considered: (1) the equipartition hypothesis is verified; (2a) it is not verified and B is constant across the cavity; (2b) it is not and CRE density is constant across the cavity. Solid lines refer to M33, while dot-dashed lines show the bounds obtainable—under the same physical hypothesis—for the MW (as in Borriello et al. 2009).
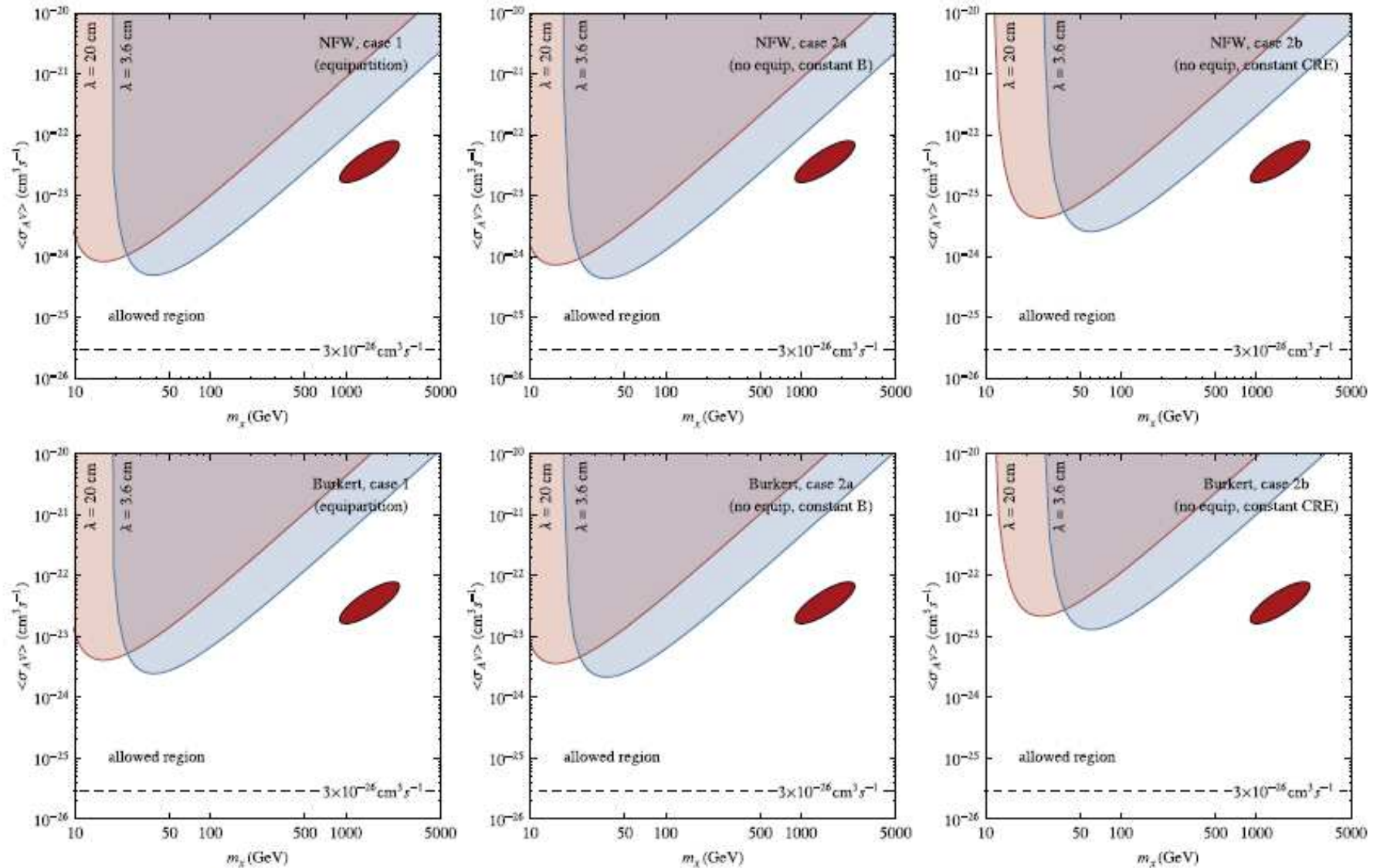
Figure 4. Same as in Figure 3 but for DM particles fully annihilating into $\mu^+\mu^-$ couples. This time the benchmark case is represented by the Pamela/*Fermi* LAT/Hess favored region (as in Meade et al. 2009) corresponding to the elliptical spot centered at about 10^3 GeV and 10^{-23} cm^3 s^{-1}.

Perspectives

Among ground-based telescopes, highest resolution (0".03) and sensitivity (0.060 mJy) observations at high frequencies ($v \sim 100$ GHz) will be achieved by the Atacama Large Millimeter Array (ALMA). In addition Rotation Measurements Synthesis (Heald et al. 2000) at as many wavelengths as possible will lead to a more precise magnetic field study, hopefully removing the degeneracy of possibilities shown above.

Such a high angular resolution could improve our results. In fact if one can identify a small region inside the cavity from which one detects a vanishing flux (within the experimental sensitivity), this naturally results in a significant improvement of our bounds.
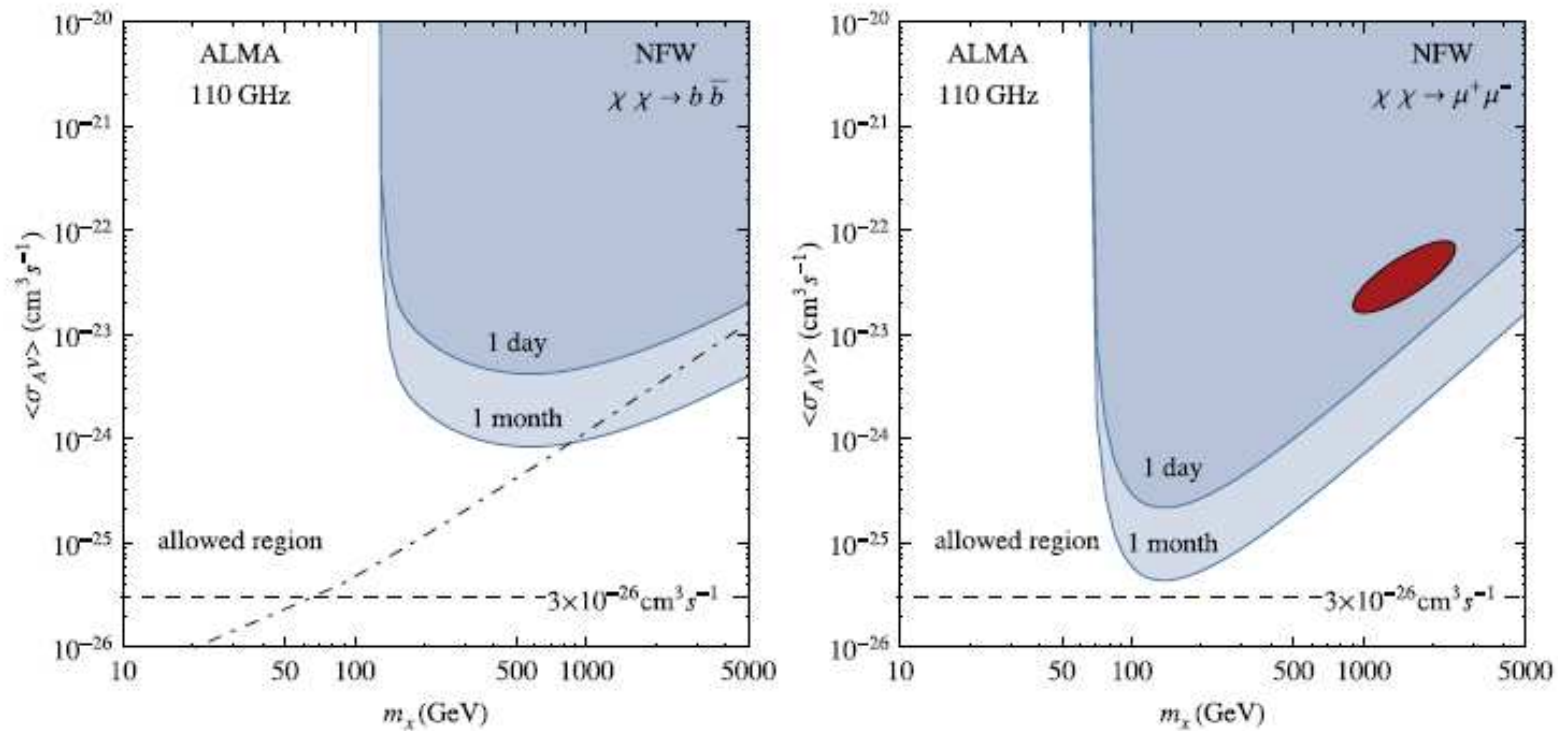
Figure 5. Exclusion plots corresponding to a null detection (within the experimental sensitivity) radio flux. The left panel refers to DM particles annihilating into $b\bar{b}$ quarks derived for 1 day and 1 month of observation. The dot-dashed line represents the forecast (at 5σ) for 5 years of *Fermi* LAT data taking obtained by means of Galprop for optimized parameters (see Baltz et al. 2008 for details). The right panel refers instead to annihilation into $\mu^+\mu^-$. The exclusion regions are superimposed to the ellipse favored by Pamela/*Fermi* LAT/Hess data (see Meade et al. 2009).

Results for M33

- The comparison of the expected DM-induced emission with radio continuum observations, especially focused on a particular low emitting *radio cavity*, allows to put bounds in the m_χ–$<\sigma_A v>$ plane.

- Not tailored archival data allow to put bounds comparable with ones obtainable form MW. This suggests the possibility that focused observations could gain a great predictive power.

- We have considered an optimistic scenario where a high-resolution radio telescope like ALMA does not detect any flux (within the experimental sensitivity) in a region inside the radio cavity. In this case, the bounds we can derive on WIMPs parameters are better than the corresponding *Fermi* LAT forecast in the case of heavy WIMPs decaying into hadrons. Assuming instead annihilation into muons we could be able to rule out the region favored by Pamela/*Fermi* LAT/Hess in a single day of observation.